

# Perforated Sheets Exhibiting Negative Poisson's Ratios\*\*

By Joseph N. Grima\* and Ruben Gatt

*Sheets made from readily available conventional materials containing diamond or star shaped perforations are shown to exhibit various Poisson's ratio values which could also be negative (auxetic). This behavior may be exhibited in both tension and compression and can be explained through models based on "rotating rigid units." This provides an easy manner for the manufacture of auxetic or conventional systems at any scale which can be tailor made to exhibit particular values of the Poisson's ratio.*

The extent of deformations that a material undergoes when it is uniaxially stretched or compressed are quantified through the Poisson's ratio, a property which is positive for most conventional materials. However, it is well known that Poisson's ratio needs not be always positive and the classical theory of elasticity suggests that the Poisson's ratio of isotropic materials can assume values within the range of  $-1-0.5$ , which range is even wider for orthotropic and anisotropic materials. In fact, negative Poisson's ratios (auxetic behavior<sup>[1-3]</sup>) has now been discovered or introduced in a wide range of naturally occurring or man-made materials<sup>[1-23]</sup> including foams,<sup>[2,4,5]</sup> polymers,<sup>[1,6-9]</sup> metals,<sup>[10]</sup> silicates,<sup>[11,12]</sup> and zeolites.<sup>[13,14]</sup> Furthermore, various model structures and mechanisms which exhibit negative Poisson's ratio have been proposed including models based on re-entrant units,<sup>[1,15]</sup> rotating rigid units<sup>[16-18]</sup> chiral systems,<sup>[19-21]</sup> and systems incorporating circular holes which exhibit Poisson's ratio in compression.<sup>[22]</sup> These materials and structures have been shown to exhibit several enhanced macroscopic properties ranging from enhanced resistance to indentation<sup>[3]</sup> to smart filtration<sup>[13]</sup> or increased vibration and acoustic absorption properties.<sup>[23]</sup> Unfortunately, despite all of these developments, the availability of materials and structures which exhibit negative Poisson's ratios is still very limited, mainly as a result of the fact that most auxetics discovered so far are

difficult or expensive to manufacture on a large scale; only exhibit negative Poisson's ratio for stretching in very particular directions (e.g., the zeolites in the natrolite group<sup>[14]</sup>) and/or only exhibit negative Poisson's ratio in compression (e.g., Bartoldi's systems incorporating circular holes<sup>[22]</sup> which systems work because of "reversible" large transformations which occur to the original geometry because of mechanical instabilities,<sup>[23,24]</sup> something that has also been observed at the sub-micrometer scale.<sup>[25,26]</sup>). Here we propose a method to overcome these problems by suggesting novel auxetic systems which can operate in both tension and compression that can be cheaply manufactured from readily available conventional sheets of material having thickness  $z$  by simply introducing perforations of particular shapes (e.g., diamond-shaped or star-shaped perforations, see Fig. 1)<sup>a</sup>.

To verify our hypothesis, we performed finite element (FE) simulations using the ANSYS software of cuboidal sheet made from an isotropic material having Young's modulus  $E$  and Poisson's ratio  $\nu$  in which we had introduced rhombic shaped perforations in a regular fashion as illustrated in Figure 1(a-c). These arrangements were chosen in view of the similarities they exhibit with the well known rotating squares/rectangles model which are well known for its auxetic properties. In fact, referring to Figure 1, one should note that in the limit that  $s \rightarrow 0$ , (where  $s$  represents the amount of material between each perforation) the system in Figure 1(a) (henceforth referred to as system **A**) and Figure 1(b) (henceforth referred to as system **B**) reduce to the connected squares geometry, a system which is predicted to

[\*] Prof. J. N. Grima, R. Gatt  
Faculty of Science, University of Malta  
Msida MSD 2080, Malta  
E-mail: joseph.grima@um.edu.mt

[\*\*] Acknowledgments: The authors would like to gratefully acknowledge the help provided by Elizabeth R. Grima and Maria Saliba.

<sup>a</sup>Note that a similar effect can be achieved through the introduction of rigid shapes in a soft matrix (the soft material replaces the void space and the hinges).

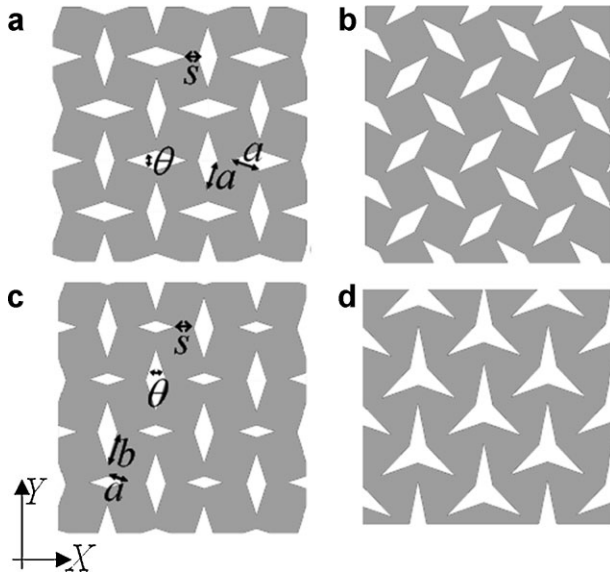


Fig. 1. Examples of perforated sheets which may exhibit negative Poisson's ratio: (a, b) systems A and B, respectively having diamond-shaped inclusions of the same size which are meant to resemble the rotating squares model; (c) system C having diamond-shaped inclusions of two different sizes which is meant to resemble the Type I rotating rectangles model; (d) a system with a star-shaped inclusion meant to resemble the rotating triangles model. Note that the systems in (a) and (b) represent the same structure having different orientation.

exhibit Poisson's ratios of  $-1$  should the squares remain rigid but simply rotate relative to each other. (The system in Fig. 1(b) is the same as the system in Figure 1(a) rotated by  $45^\circ$ ). Similarly, the system in Figure 1(d) represents the rotating triangles model whilst the system in Figure 1(c) (henceforth referred to as system C) reduces to the Type I rotating rectangles which exhibit Poisson's ratios of:

$$\nu_{xy} = (\nu_{yx})^{-1} = \frac{a^2 \cos^2(\frac{\theta}{2}) - b^2 \sin^2(\frac{\theta}{2})}{a^2 \sin^2(\frac{\theta}{2}) - b^2 \cos^2(\frac{\theta}{2})} \quad (1)$$

where  $a$  and  $b$  are the sides of the rectangles, and  $\theta$  represents the angle between the rectangles. Note that these mechanisms involving rotating rigid units have been found to be responsible for negative Poisson's ratios in a wide range of materials including zeolites.<sup>[13,14]</sup>

Four sets of simulations were performed, two where systems A and B shown in Figure 1(a, b), respectively where stretched in the Y direction and another two where system C [shown in Fig. 1(c)] was stretched first in the X and then in the Y direction. All systems were constructed by inserting a pre-defined number of perforations on a 2D sheet of an isotropic material having its materials properties similar to those of rubber i.e.,  $E = 2 \times 10^6$  Pa and  $\nu = 0.47$ . The dimensions of the sheet ( $l_x \times l_y$ ) were set to about  $60 \text{ mm} \times 60 \text{ mm}$  where the exact dimension where chosen in such a way so as to ensure periodicity. In all sets of simulations,  $\theta$  was given values  $10^\circ, 20^\circ, 30^\circ, \dots, 90^\circ$  and  $s$  was given values of 0.1, 1, 2, 3, and 4 mm. In the case of systems A and B, the length  $a$  was arbitrarily set at 5 mm whilst in the case of system C, the length  $a$  was set at 5 mm whilst  $b$  was set at 7 mm. Note that these

dimensions may easily be converted to calculate the volume fraction  $V_f$  of some particular system through the equation:

$$V_f = 1 - 2(A_1 + A_2)A^{-1} \quad (2)$$

where  $A$  is the area of the unit cell given by:

$$A = 4 \left[ s + a \sin\left(\frac{\theta}{2}\right) + b \cos\left(\frac{\theta}{2}\right) \right] \times \left[ s + a \cos\left(\frac{\theta}{2}\right) + b \sin\left(\frac{\theta}{2}\right) \right] \quad (3)$$

and  $A_1$  and  $A_2$  represent the areas of the holes (which are of the same size when  $a = b$ ) which are given by:

$$A_1 = 2a^2 \sin\left(\frac{\theta}{2}\right) \cos\left(\frac{\theta}{2}\right) \quad \text{and} \quad A_2 = 2b^2 \sin\left(\frac{\theta}{2}\right) \cos\left(\frac{\theta}{2}\right) \quad (4)$$

These models were then meshed using PLANE82 elements (an 8 node quadratic element) and solved under the constrain of a 1 mm displacement in the direction of stretching of an edge perpendicular to this direction. This corresponds to applied uniaxial strains in the region of 1.40%–2.07%. The Poisson's ratios of these systems were then calculated by averaging the displacements of the nodes at the edges of the model which were initially parallel to the direction of stretching. These simulations were then repeated in compression. Note that this method of measuring strains and these boundary conditions used have been chosen so as to represent as much as possible what is occurring in real systems.

The results of these simulations in tension are summarized in Figure 2 and clearly suggest that these systems can exhibit a wide range of Poisson's ratio which may be positive, negative (auxetic), or zero. It is also worth to note that in some cases, the predicted positive values of the Poisson's ratio significantly exceed the magnitude of the Poisson's ratio of material used (in this case rubber). Similar properties were observed in compression.

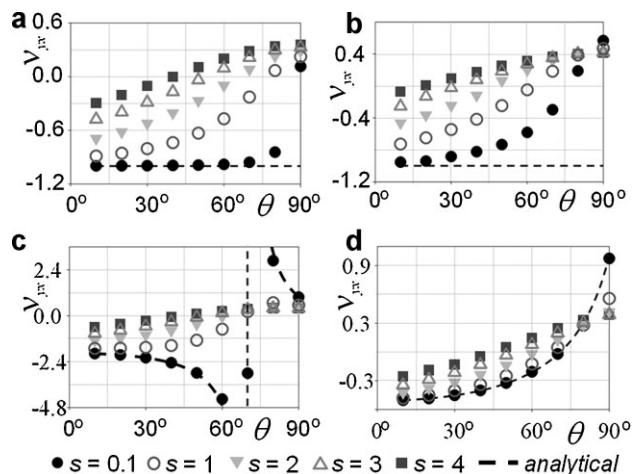


Fig. 2. The Poisson's ratios as simulated by ANSYS, showing the results obtained for (a) the system A [see Fig. 1(a)] for loading in the Y-direction, (b) system B [see Fig. 1(b)] for loading in the Y-direction (c) system C [see Fig. 1(c)] for loading in the Y-direction and (d) system C [see Fig. 1(c)] for loading in the X-direction. (The angle  $\theta$  is measured in degrees and  $s$  in mm.)

In particular, referring to Figure 2(a), we note that when  $s = 0.1$  mm, the Poisson's ratio of system **A** tend to values of  $-1$  for the smaller values of  $\theta$ . This confirms that this system is indeed mimicking the behavior of the "rotating squares" model which is known to exhibit Poisson's ratios of  $-1$  in the idealized scenario when the squares are perfectly rigid. However, we note that even this system exhibits significant deviations from the idealized scenario as  $\theta$  approaches  $90^\circ$ . This behavior may be explained by the fact that in real systems, the rotating squares mechanism is accompanied by other deformation mechanisms which are not necessarily conducive to negative Poisson's ratios (e.g., deformations of the squares themselves). If one assumes that these other mechanisms collectively result in Poisson's ratios of  $\nu^{\text{oth}}$  and Young's moduli  $E^{\text{oth}}$  whilst the idealized rotating squares has Poisson's ratio of  $\nu^{\text{RS}} = -1$  and Young's moduli  $E^{\text{RS}}$  which is given by:

$$E^{\text{RS}} = k_h \frac{8}{a^2 Z} \frac{1}{[1 - \sin(\theta)]} \quad (5)$$

where  $a$  is the length of the sides of the squares,  $\theta$  the angle between the squares,  $z$  the dimension in the third direction, and  $k$  is a stiffness constant which describes the stiffness of the hinge between the squares, then the Poisson's ratio of the real system, may be approximated by:

$$\frac{\nu^{\text{obs}}}{E^{\text{obs}}} = \frac{\nu^{\text{RS}}}{E^{\text{RS}}} + \frac{\nu^{\text{oth}}}{E^{\text{oth}}} \quad (6)$$

Under these approximations, we note that from Equation 5,  $E^{\text{RS}} \rightarrow \infty$  as  $\theta \rightarrow 90^\circ$  and thus  $\frac{\nu^{\text{RS}}}{E^{\text{RS}}} \rightarrow 0$  with the result that  $\nu^{\text{obs}} \rightarrow \nu^{\text{oth}}$  rather than the value of  $-1$  predicted for the idealized rotating squares model. Such behavior where the Poisson's ratios increase (i.e., become less negative) as  $\theta$  increases is observed for all values of  $s$  modeled and may be explained through similar arguments. It is also interesting to note that the data in Figure 2(a) also suggests that as  $s$  increases, the Poisson's ratios become less negative for any given value of  $\theta$ . This can be explained by the facts that these conformations lose their resemblance to the idealized rotating squares mechanisms as  $s$  increases. Furthermore, we note that the value of  $s$  may be directly related to the magnitude of the stiffness of the hinge which in turn results in higher values of  $E^{\text{RS}}$  thus effectively lowering the contribution of the rotating squares mechanism. All this may be observed if one looks at the deformed shape of these conformations as simulated by ANSYS [see Fig. 3(a, b)].

We note that similar behavior is exhibited for system **C** illustrated in Figure 1(c) when loaded in the  $X$  or  $Y$  directions, although this time the resemblance is to the idealized "Type I rotating rectangles" rather than the rotating squares. One should note that system **C** offers a wider range of Poisson's ratio values when compared to system **A** (the "squares"). In fact, the Poisson's ratios recorded in Figure 2(c, d) were as low as  $-4.37$  and as high as  $+2.86$ , a value which is even higher than that of rubber itself. Various conformations also exhibit Poisson's ratio values which are close to 0, a property which is

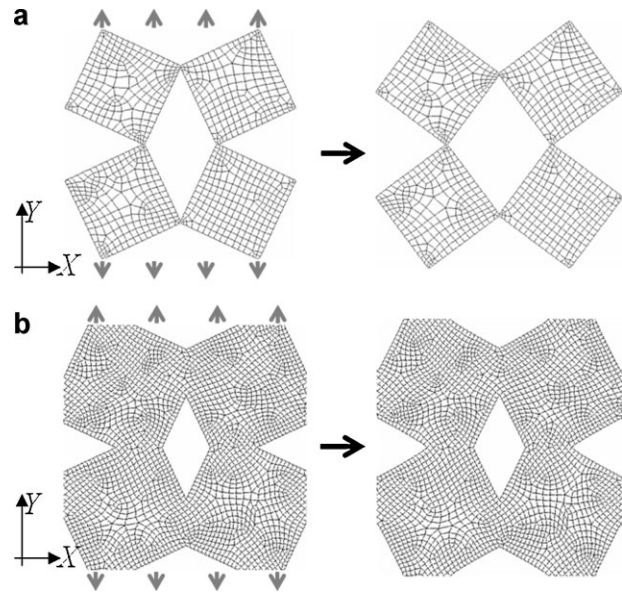


Fig. 3. Magnified part of system **A** [see Fig. 1(a)] showing the undeformed conformation (left) and deformed conformation as simulated by ANSYS (right) when  $\theta = 50^\circ$ ,  $a = 5$  mm and (a)  $s = 0.1$  mm, (b)  $s = 4$  mm. Note that in (a) the main deformation mechanism is the relative rotations of the squares which results in negative Poisson's ratio whilst the deformations in (b) are dominated by the other deformation mechanisms with the net result that the Poisson's ratio is positive.

important in its own accord (these are systems which neither get fatter nor thinner when stretched or compressed).

If we now look at Figure 2(b) we note that system **B** [Fig. 1(b)] exhibits similar trends in its Poisson's ratios to system **A** [Fig. 1(a)] although the Poisson's ratios of the various conformations of system **B** are less negative when compared to the equivalent conformations of system **A**. Bearing in mind that the systems **A** [Fig. 1(a)] and **B** [Fig. 1(b)] are in fact the same system rotated by  $45^\circ$  to each other and noting that all conformations which in Figure 2(b) are shown to exhibit negative Poisson ratio will also exhibit negative Poisson's ratio in Figure 2(a), then it becomes clear that these conformations will exhibit negative Poisson's ratio for loading both on-axis and  $45^\circ$  off-axis. This is very significant and of practical importance since the conformation in Figure 2(b) is likely to correspond to the least auxetic system,<sup>[28]</sup> i.e., one may conclude that the systems in Figure 1(a) or (b) are likely to be auxetic for loading in any off-axis direction.

It is important to note that the simulations presented here correspond to small scale deformations. If the systems had been stretched or compressed further, one would expect that the Poisson's ratio of our proposed systems will increase (i.e., become less negative). For example, we envisage that at very high strains, the proposed "rotating rigid units" mechanism will become less significant when compared to other modes of deformation to the extent that systems which are auxetic at small strains will start to exhibit conventional behavior.

It is also important to note that the systems modeled here represent a highly idealized scenario corresponding to structures made from a rubbery material having an infinite thickness  $z$  in the third dimension. In reality, the overall

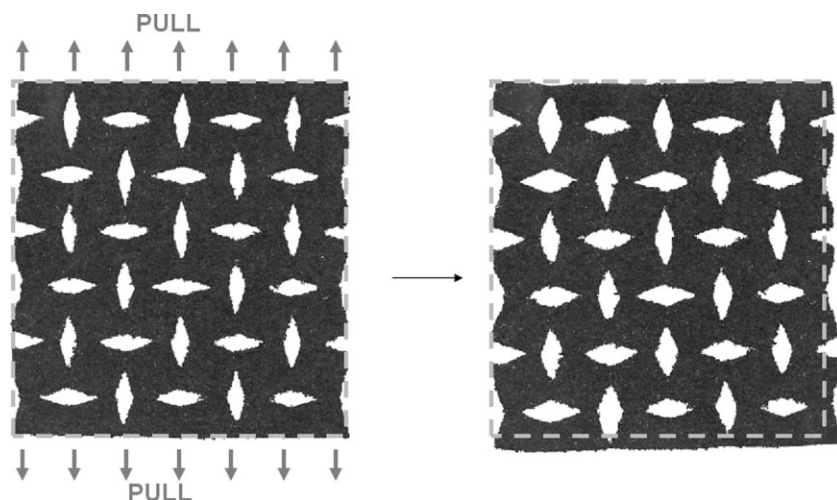


Fig. 4. An experimental verification of this model using a material that is commonly used for disposable carpets, showing that the squares are rotating relative to each other when stretched. Note that this system was too thin to permit testing in compression.

properties of the system will depend on the properties of the material used in the manufacture of the sheets. More importantly, sheets having a finite thickness will tend to deform out of plane, a property which will affect the Poisson's ratio in the plane<sup>b</sup>. We also note that although our simulations suggest that our systems work in both tension and compression, in practice one is likely to find that systems in compression would need to have a considerable thickness in the third dimension to work effectively. In fact, a model we produced using material that is commonly used for disposable carpets exhibited some out of plane deformations when stretched although these deformations still permitted the system to exhibit a negative Poisson's ratios in the plane when stretched thus confirming the predictions of our simulations (see Fig. 4). Here one should note that although the system in Figure 4 and the modeling presented here corresponds to structures having dimensions in the mm scale, this effect is scale independent and may be implemented at any lengthscale including the microscale (by introducing micro-perforations) so as to produce a system which may be classified as a "material" rather than a "structure."

Before we conclude, it is important to note that the work presented here complements recent work done by Bertoldi *et al.* and brings to light the mechanism which is resulting in the negative Poisson's ratios in Bertoldi's systems. In fact, if one compares the systems presented here (which operate in both tension and compression) to Bertoldi's compressed systems (Bertoldi's systems need to be pre-compressed to exhibit negative Poisson's ratios<sup>[22]</sup>) one will be able to observe that both systems are achieving negative Poisson's ratios through the rotating rigid unit mechanisms which are

<sup>b</sup>Note that such out of plane deformations result in an out of plane negative Poisson's ratio  $\nu_{zi}$  where  $i$  represents the direction of loading in the plane of the structure whilst  $z$  is the direction perpendicular to the plane of the structure.

discussed elsewhere.<sup>[16,17,28–30]</sup> In fact, it should be emphasized that the main requirement for such systems to exhibit negative Poisson's ratios is to have "holes" of the right shape and inserted in such a way that the resulting structure mimics one of the known auxetic models (e.g., star shaped holes arranged as in Figure 1(d) which results in a structure which mimics Grima's "rotating triangles" model).

To conclude, through this work we have shown that systems constructible at any lengthscale which exhibit a wide range of Poisson's ratio in both tension and in compression (assuming they are thick enough not to pucker) which can even be negative or zero can be achieved by sheets by introducing appropriate perforations. Given the ease by which such systems can be

manufactured, recent advances in the field of manufacturing (e.g., recent work reporting fabrication of two and three-dimensional structures based on interference lithography<sup>[31]</sup>) and the wide range of applications for auxetic systems, we hope that this work will encourage further developments in this direction and facilitate the mass-production of auxetics.

Received: January 4, 2010

Final Version: April 8, 2010

- [1] K. E. Evans, M. A. Nkansah, I. J. Hutchinson, S. C. Rogers, *Nature* **1991**, 353, 124.
- [2] R. Lakes, *Science* **1987**, 235, 1038.
- [3] K. E. Evans, *Endeavour* **1991**, 15, 170.
- [4] J. N. Grima, D. Attard, R. Gatt, R. N. Cassar, *Adv. Eng. Mater.* **2009**, 11, 533.
- [5] N. Chan, K. E. Evans, *J. Cell. Plast.* **1998**, 34, 231.
- [6] K. E. Evans, B. D. Caddock, *J. Phys. D: Appl. Phys.* **1989**, 22, 1883.
- [7] C. B. He, P. W. Liu, A. C. Griffin, *Macromolecules* **1998**, 31, 3145.
- [8] J. N. Grima, K. E. Evans, *Chem. Commun.* **2000**, 1531.
- [9] V. R. Simkins, N. Ravirala, P. J. Davies, A. Alderson, K. L. Alderson, *Phys. Status Solidi B* **2008**, 245, 598.
- [10] R. H. Baughman, J. M. Shacklette, A. A. Zakhidov, S. Stafstrom, *Nature* **1998**, 392, 362.
- [11] A. Yeganeh-Haeri, D. J. Weidner, D. J. Parise, *Science* **1992**, 257, 650.
- [12] J. N. Grima, R. Gatt, A. Alderson, K. E. Evans, *J. Mater. Chem.* **2005**, 15, 4003.
- [13] J. N. Grima, R. Jackson, A. Alderson, K. E. Evans, *Adv. Mater.* **2000**, 12, 1912.
- [14] J. N. Grima *et al.*, *Appl. Phys.* **2007**, 101, 086102.
- [15] I. G. Masters, K. E. Evans, *Compos. Struct.* **1996**, 35, 403.
- [16] J. N. Grima, K. E. Evans, *J. Mater. Sci. Lett.* **2000**, 19, 1563.

- [17] Y. Ishibashi, M. J. Iwata, *J. Phys. Soc. Jpn.* **2000**, *69*, 2702.
- [18] J. N. Grima, K. E. Evans, *J. Mater. Sci.* **2006**, *41*, 3193.
- [19] D. Prall, R. S. Lakes, *Int. J. Mech. Sci.* **1996**, *39*, 305.
- [20] F. Scarpa, *et al. Compos. Part A* **2007**, *38*, 280.
- [21] K. W. Wojciechowski, *Phys. Lett. A* **1989**, *137*, 60.
- [22] B. Bertoldi, P. M. Reis, S. Willshaw, T. Mullin, *Adv. Mater.* **2009**, *27*, 1.
- [23] F. Scarpa, G. Tomlinson, *J. Sound Vib.* **2000**, *230*, 45.
- [24] T. Mullin, S. Deschanel, K. Bertoldi, M. C. Boyce, *Phys. Rev. Lett.* **2007**, *99*, 084301.
- [25] K. Bertoldi, M. C. Boyce, S. Deschanel, S. M. Prange, T. Mullin, *J. Mech. Phys. Solids* **2008**, *56*, 2642.
- [26] Y. Zhang, E. A. Matsumoto, A. Peter, P. C. Lin, R. D. Kamien, S. Yang, *Nano Lett.* **2008**, *8*, 1192.
- [27] J. H. Jang, C. Y. Koh, K. Bertoldi, M. C. Boyce, E. L. Thomas, *Nano Lett.* **2009**, *9*, 2113.
- [28] J. N. Grima, *Phys. Status Solidi B* **2007**, *244*, 866.
- [29] J. N. Grima, P.-S. Farrugia, R. Gatt, D. Attard, *Phys. Status Solidi B* **2008**, *245*, 521.
- [30] J. N. Grima, K. E. Evans, *J. Mater. Sci.* **2006**, *41*, 3193.
- [31] A. F. Lasagni, B. S. Menéndez-Ormaza, *Adv. Eng. Mater.* in press (DOI: 10.1002/adem.200900221).

## Life's Simple Pleasures!



No need to waste precious time looking for the right information – Register now for the free **Wiley-VCH Alerting Service**.

**It's simple – and it's fast.**

To receive regular news per e-mail tailored precisely to your needs and interests, just fill in the registration form at [www.wiley-vch.de/home/pas/](http://www.wiley-vch.de/home/pas/)

